Journal of Fluorine Chemistry 129 (2008) 720–724

Contents lists available at ScienceDirect

Journal of Fluorine Chemistry

journal homepage: www.elsevier.com/locate/fluor

Short communication

Reaction of graphite fluoride with NaOH–KOH eutectic

Athanasios B. Bourlinos [a,*], Vasilios Georgakilas [a], Radek Zboril [b], Dalibor Jancik [b], Michael A. Karakassides [c], Andreas Stassinopoulos [d], Demetrios Anglos [d], Emmanuel P. Giannelis [e,*]

[a] Institute of Materials Science, NCSR "Demokritos", Ag. Paraskevi Attikis, Athens 15310, Greece
[b] Departments of Physical Chemistry and Experimental Physics, Palacky University, Olomouc 77146, Czech Republic
[c] Department of Materials Science and Engineering, University of Ioannina, 45110 Ioannina, Greece
[d] Institute of Electronic Structure and Laser, Foundation for Research and Technology-Hellas, P.O. Box 1385, GR-711 10 Heraklion, Crete, Greece
[e] Department of Materials Science and Engineering, Cornell University, Ithaca, NY 14853, USA

ARTICLE INFO

Article history:
Received 6 May 2008
Received in revised form 28 May 2008
Accepted 29 May 2008
Available online 7 June 2008

Keywords:
Graphite fluoride
Eutectic NaOH–KOH
Graphitization
Water-soluble carbon
Fluorescence
Carbon morphology

ABSTRACT

Graphite fluoride has been generally considered chemically inert against strong alkalis under ambient conditions. In the present study we demonstrate that treatment of graphite fluoride with eutectic NaOH–KOH mixture at 250 °C induces dramatic structural and textural changes in the solid as evidenced by XRD, FT-IR, Raman, UV–vis absorption and fluorescence and microscopy techniques (TEM, AFM). The reaction proceeds in the molten state leading to water-soluble, graphitized carbon particles which unlike graphite fluoride, adopt a variety of morphologies, like platy, tetragonal, triangular, discoid and spherical. The resulting carbon particles are dispersible in water and fluoresce under UV excitation.

1. Introduction

Graphite fluoride is a well-known covalent derivative of graphite with interesting lubricating, hydrophobic and electrochemical properties [1]. Depending on the preparative conditions, different fluorine to carbon atomic ratios can be achieved with the most representative example being the carbon monofluoride (CF_x, $x \sim 1$). This particular grey solid lacks the aromatic character of graphite and has puckered cyclohexane ring structure with fluorines substituted above and below the rings [2]. Besides the stability of the C–F bond, the compound still undergoes fluorine substitution reactions to form various reconstructed derivatives, e.g. hydrogenated, oxygenated or alkylated [3–5]. To that end, the reaction between strong hydroxides and graphite fluoride is of particular interest, especially considering that the fluorine atom and the hydroxyl group are isoelectronic and have similar polarity. Generally, fluorinated graphites are stable in concentrated alkaline media under ambient conditions with the reaction being slow and proceeding mainly at the solid–liquid interface [6]. Thus, more drastic conditions are required for further reaction, provided that one avoids the intrinsic decomposition of the solid. Here we report the reaction of as purchased graphite fluoride powder (CF_x, $x \sim 1$) with excess of eutectic NaOH–KOH melt at 250 °C (Scheme 1). The strongly basic (molten hydroxide) flux provides a better kinetics at relatively low temperature. The reaction results in water-soluble, graphitized carbon particles that adopt various morphologies as a result of the alkali activation. The resulting carbon particles are dispersible in water and fluorescence upon excitation in the UV.

2. Results and discussion

The reaction between graphite fluoride (CF) and excess alkali hydroxide takes place at 250 °C under molten conditions, i.e. in a strongly basic flux, and is believed to proceed in two stages. The first one involves nucleophilic substitution [5] of the fluorine atoms by the isoelectronic hydroxyl groups leading to the formation of a thermally unstable polyhydroxy network. In the second stage this intermediate undergoes oxygen elimination and in turn graphitization, analogous with graphite oxide [7] and carbohydrates [8]. A possible reduction of graphite fluoride to carbon by the hydroxide ions cannot be also ruled out [9,10]. Residual hydroxyl groups near the edges of the graphitized layers render the carbon particles soluble in water thus providing a black colloid with concentration 0.2 mg ml^{-1} (Scheme 1). Generally,

* Corresponding authors. Tel.: +30 210 6503309; fax: +30 210 6519430.
E-mail addresses: bourlinos@ims.demokritos.gr (A.B. Bourlinos), epg2@cornell.edu (E.P. Giannelis).

0022-1139/$ – see front matter © 2008 Elsevier B.V. All rights reserved.
doi:10.1016/j.jfluchem.2008.05.020

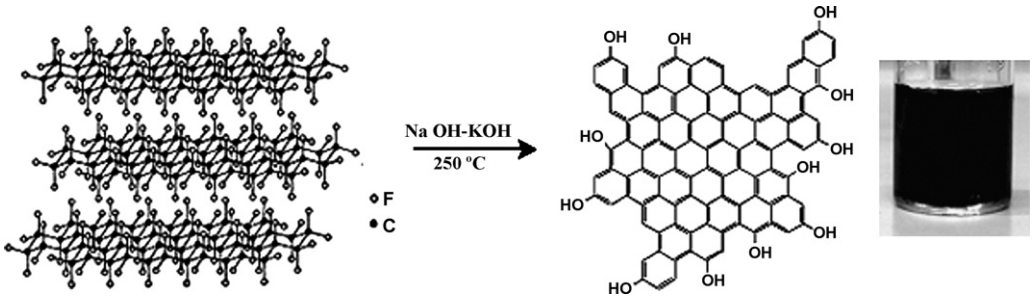

Scheme 1.

graphite edge planes have been studied to a lesser extent and the dominating opinion is that the discontinuity of graphite planes inevitably exists at the edge [11,12]. Accordingly, Scheme 1 depicts a simplified structural model for the derived carbon showing in a qualitative way bulk graphitization and the type of edge functionalization. Note that no decomposition was observed by merely heating graphite fluoride at 250 °C (based on XRD and FT-IR measurements). Lastly, the eutectic NaOH–KOH mixture provides a liquid at relatively low temperature, unlike the individual components that melt above 300 °C. The latter is important because reaction temperatures higher than 250 °C lead to insoluble carbon due to complete de-oxygenation.

The XRD measurements (Fig. 1) show a *d*-spacing of 0.65 nm for the starting graphite fluoride [5]. After reaction, a peak corresponding to a *d*-spacing of 0.34 nm appears consistent with the formation of turbostratic carbon [5,13]. The FT-IR spectrum of graphite fluoride exhibits a strong band at 1218 cm^{-1} due to the C–F stretching vibration that is completely suppressed after reaction (Fig. 1). Instead, the carbon solid, which may contain a very small fraction of residual fluorine, shows weak and broad absorptions between 900 and 1300 cm^{-1} that are characteristic of oxygen-containing functional groups (e.g. C–OH). On the basis of the XRD data, we can conclude that these groups are located at the periphery of the layers (Scheme 1). The Raman spectrum of CF contains two weak and broad bands: the tangential G-mode (1580 cm^{-1}) and the disorder-induced D-mode (1320 cm^{-1}) [5]. After reaction, the D and G bands sharpen significantly while their frequency shifts upward, consistent with graphitization [5] (Fig. 2).

According to light scattering measurements the average particle size is 85 nm with a relatively narrow size distribution (Fig. 3). Optical spectroscopy clearly differentiates between the starting graphite fluoride and the derived carbon product (Fig. 3). The UV–vis absorption spectrum of a dilute suspension of graphite fluoride in ethanol shows mainly a gradually increasing background from the visible to the UV due to particle scattering. On the other hand, a dilute colloidal dispersion of the carbon particles in water exhibits a distinct absorption band at 260 nm and a long absorption tail extending beyond 800 nm (presumably hiding also some scattering component). Given the complexity of the system one cannot unambiguously assign the 260 nm feature to a specific molecular structure. However, it is worth noting that carbon nanoparticles produced through electrochemistry from multi-walled carbon nanotubes show a clear absorption band at 270 nm [14].

The colloidal carbon particles show fluorescence emission when excited in the UV [14–17] (Fig. 3). In fact the fluorescence emission spectra show two bands at 340 nm and 420 nm. The intensity of these bands varies with excitation wavelength and this becomes quite evident in the fluorescence excitation spectra. The emission band peaking at 340 nm appears for excitations below 300 nm and corresponds to an absorption feature at 280 nm while the emission band peaking at 420 nm appears for excitations below 400 nm and corresponds to an excitation profile with two distinct maxima, one at 310 nm and one at 260 nm the latter corresponding to the band seen in the absorption spectrum. Excitation of the solution in the visible (>400 nm) results in weak

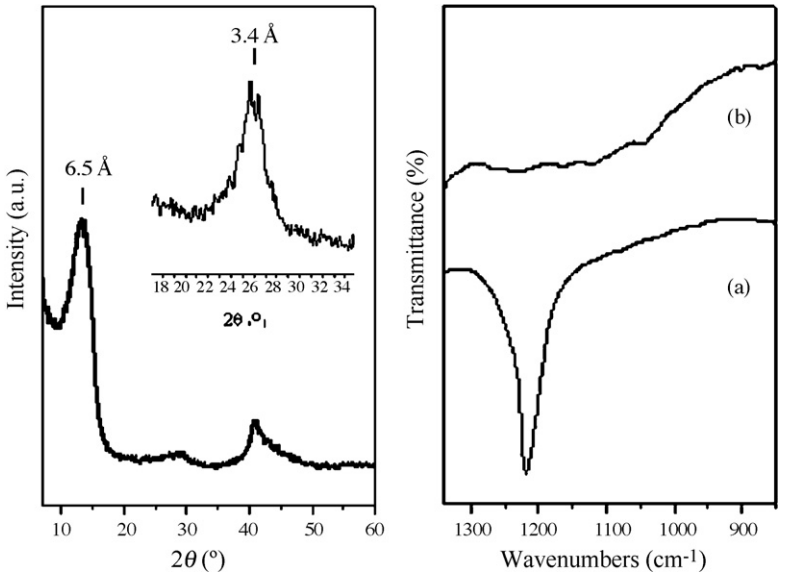

Fig. 1. Left: XRD patterns of graphite fluoride and of the derived carbon material (inset). Right: FT-IR spectra of graphite fluoride (a) and of the resulting carbon particles (b).

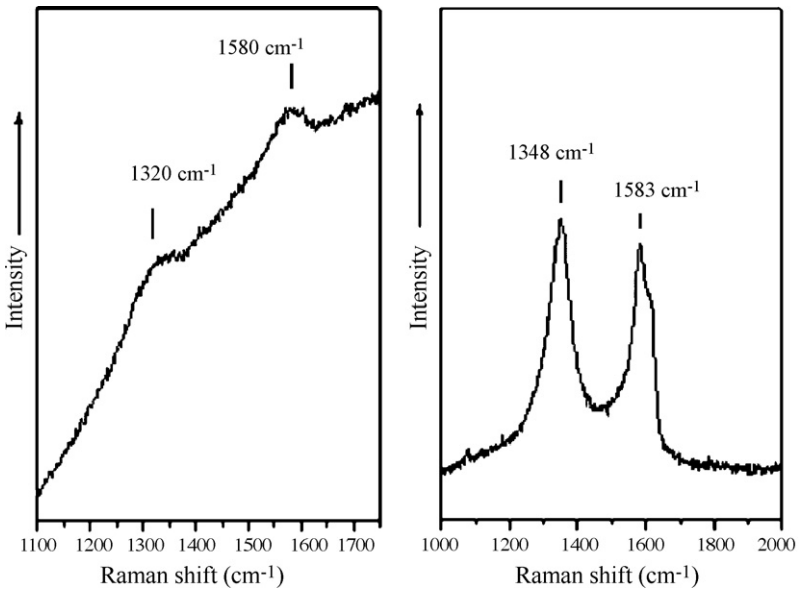

Fig. 2. Raman profiles of graphite fluoride (left) and of the derived carbon particles (right).

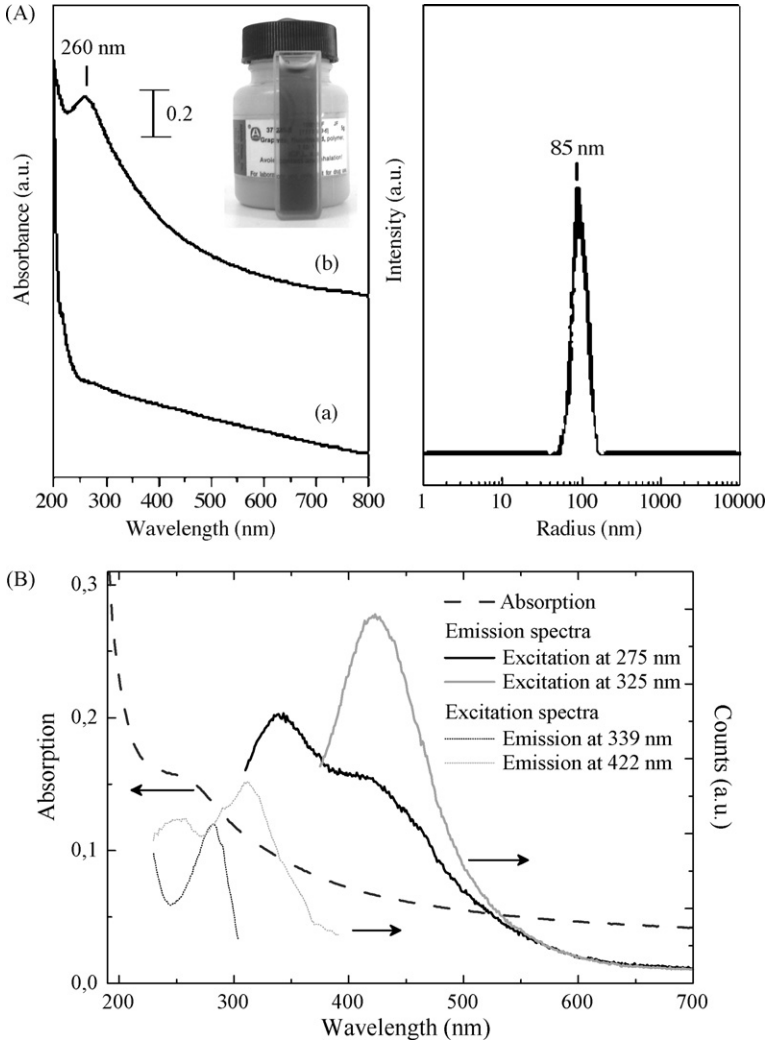

Fig. 3. (A) Left: optical spectra of a dilute suspension of graphite fluoride in ethanol (a) and of the resulting carbon particles in water (0.05 mg ml^{-1}) (b) (the absorbance in spectrum b has been scaled). The inset shows an optically transparent, dilute colloidal dispersion of the carbon particles in water. Right: light scattering size distribution for the water-soluble carbon particles. (B) Absorption (dashed line), emission (solid line) and excitation (dotted line) spectra of the water-soluble carbon particles. Note that the two absorption plots presented corresponds to different aqueous concentrations of the carbon particles.

fluorescence tails verifying that the tail in the absorption spectrum is not just due to scattering but reflects the presence of absorbing species. Clearly the fluorescence behaviour observed points towards the presence of at least two types of fluorophores in our colloidal carbon particles. The overall fluorescence quantum yield was estimated to be on the order of 0.5–1%.

TEM and AFM studies show a mixture of carbon platy particles, crystalline sheets and amorphous spheres (prevailing phase) (Fig. 4). Platy graphitized particles appear rarely in the sample (<10%). They reveal low crystallinity with many structural defects, e.g. quasi-crystalline. Optically transparent sheets of extraordinary thin crystals with tetragonal, triangular or discoid morphologies with sizes ranging from 50 to several hundreds nanometers (20–30%) are also present. These particles are actually a collection of several numbers of graphene layers (3–5), however, no single graphene crystal could be detected in the dried sample [5]. Spheres are the dominant phase in the sample (50–70%) and they are amorphous. Their size ranges between 20 and 60 nm. The globular particles are in various degrees of agglomeration, including chains. The observed morphologies and in particularly the spherical one do not exist in the starting CF, which shows instead platy microcrystals with folded edges as the predominant phase (Fig. 5). Apparently, chemical activation of carbon by the strong alkalis [18] is responsible for the observed morphologies of the carbon particles formed.

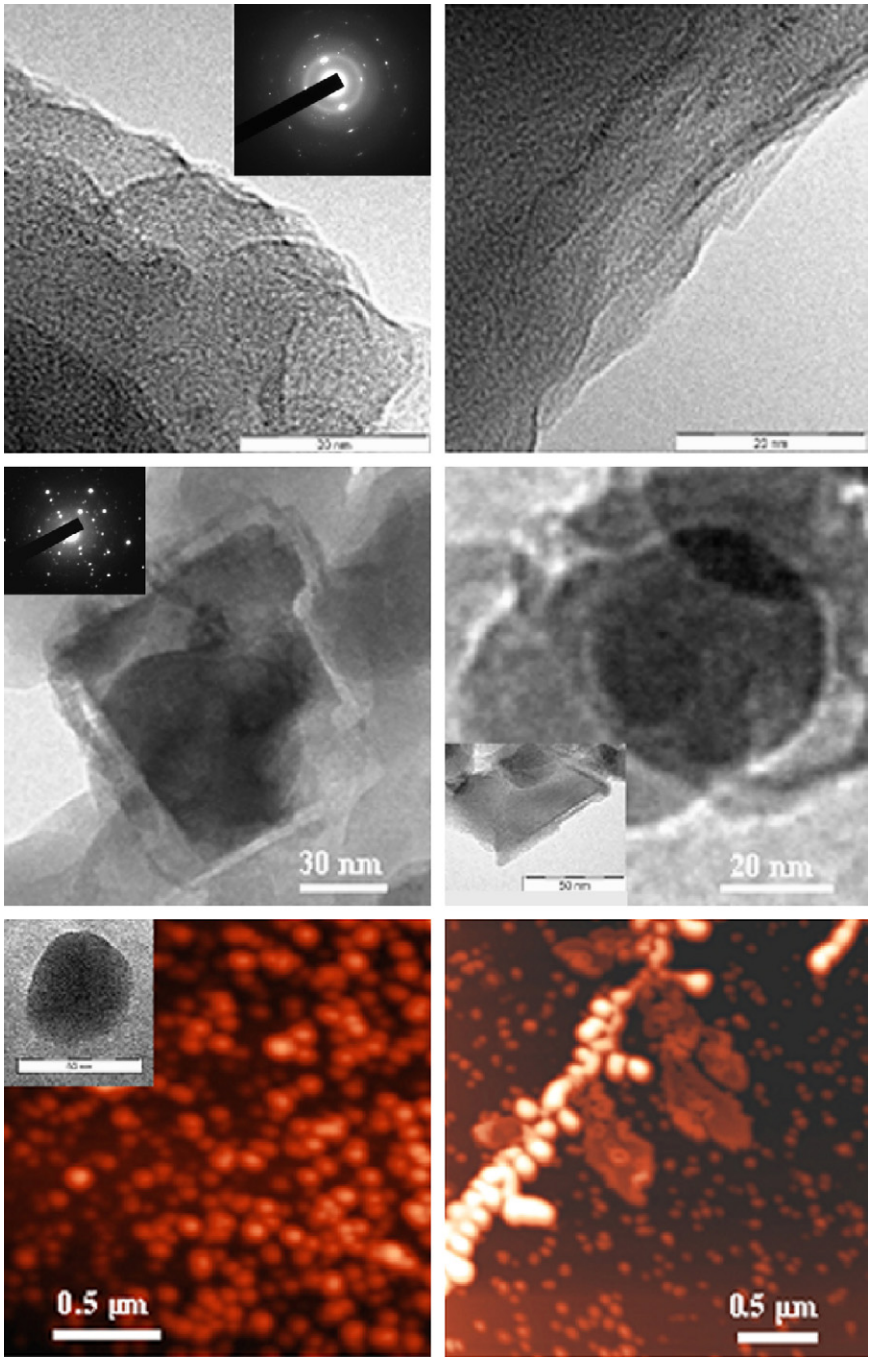

Fig. 4. Top: TEM micrographs of platy carbon particles. Middle: representative TEM pictures from tetragonal, discoid and triangular (inset) carbon particles. Bottom: AFM images of spherical carbon particles. The inset shows the TEM picture of a single carbon particle (scale bar: 40 nm).

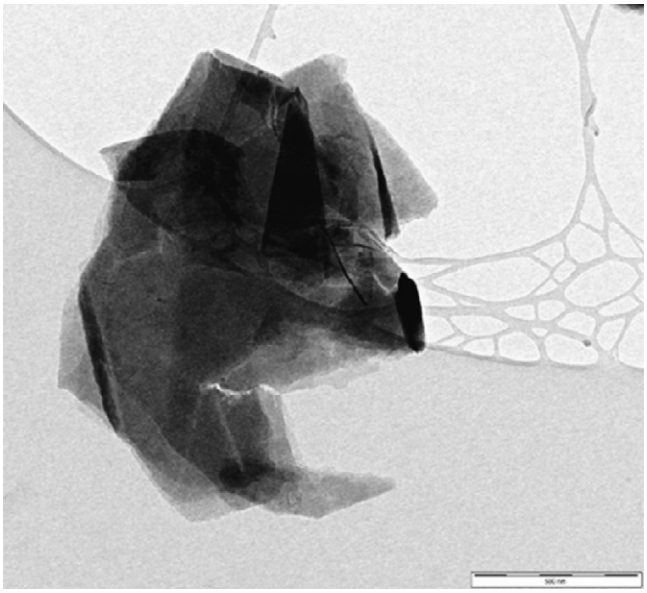

Fig. 5. TEM imaging of the starting graphite fluoride (scale bar: 500 nm).

3. Conclusions

Reaction of graphite fluoride with a strongly basic, molten hydroxide flux results in water-soluble carbon particles as a result of the alkali activation. XRD, FT-IR, Raman, UV–vis and microscopy suggest the presence of nanoscale graphitized carbon particles with various morphologies. The carbon particles are dispersible in water and fluoresce under UV excitation.

4. Experimental

Graphite fluoride powder was purchased from Aldrich (CF_x, $x \sim 1$). XRD patterns were recorded on a Siemens XD-500 diffractometer using Cu Kα radiation. The patterns were collected using background-free holders. IR measurements were made on a FT-IR spectrometer, Bruker, equinox 55/S model using KBr pellets. The Raman spectra were recorded using a Raman microscope system (Renishaw, System 1000) consisting of an optical microscope (Leica) coupled to a Raman spectrometer (532 nm). The optical absorption spectra were collected on a Cary 50 UV/Vis spectrophotometer (Varian), while fluorescence emission spectra were recorded on a Fluoromax-P fluorimeter (Jobin-Yvon). The size of the dispersed particles was measured by a dynamic light scattering apparatus (AXIOS-150/EX, Triton-Hellas) with a 30 mW laser source and a photodiode detector at an angle of 90°. TEM was carried out on a JEOL JEM 2010 microscope operated at 200 kV. AFM images were obtained with an atomic force microscope (Explorer, ThermoMicroscopes) using a mica substrate in a noncontact mode with silicon tips of the 1650-00 type and resonance frequencies ranging from 180 to 240 kHz.

For the reaction, graphite fluoride (55 mg) was blended with 1:1 (w/w) NaOH–KOH pellet mixture (2.4 g). The admixture was then heated at 250 °C for 8 h in air at a heating rate of 10 °C min^{-1}. The product was washed by suspending it in water and centrifugation at 12,000 rpm for 5 min. After repeating the washing procedure once more, the remaining solid was dispersed in water (15 ml) and filtered through a large-pore paper filter. The filtrate was left to rest for 2 days before collecting the supernatant clear colloid (0.2 mg ml^{-1}) (Scheme 1). Yield: <5%.

Acknowledgements

This work was supported by CFCI funded by DOE, the project ΠΕΝΕΔ-contract 03ΕΔ581, and the projects of the ministry of education of the Czech Republic (1M6198952901 and MSM6198959218).

References

[1] N. Watanabe, T. Nakajima, H. Touhara, Graphite Fluorides, Elsevier, Amsterdam, 1988, p. 263.
[2] N. Watanabe, S. Koyama, H. Imoto, Bull. Chem. Soc. Jpn. 53 (1980) 2731–2734.
[3] Y. Sato, H. Watano, R. Hagiwara, Y. Ito, Carbon 44 (2006) 664–670.
[4] V.N. Mitkin, N.F. Yudanov, V.V. Moukhin, V.V. Rozhkov, J. New Mater. Electrochem. Syst. 6 (2003) 103–118.
[5] K.A. Worsley, P. Ramesh, S.K. Mandal, S. Niyogi, M.E. Itkis, R.C. Haddon, Chem. Phys. Lett. 445 (2007) 51–56.
[6] D. Devilliers, H. Groult, M. Chemla, J. Fluorine Chem. 57 (1992) 73–81.
[7] Y. Matsuo, Y. Sugie, Carbon 36 (1998) 301–303.
[8] W. Xing, J.S. Xue, J.R. Dahn, J. Electrochem. Soc. 143 (1996) 3046–3052.
[9] O.G. Zarubitskii, Russ. Chem. Rev. 49 (1980) 536–548.
[10] Y. Lu, J. Liu, G. Diffee, D. Liu, B. Liu, Tetrahedron Lett. 47 (2006) 4597–4599.
[11] S.V. Rotkin, Y. Gogotsi, Mater. Res. Innovat. 5 (2002) 191–200.
[12] L.G. Cançado, M.A. Pimenta, B.R.A. Neves, M.S.S. Dantas, A. Jorio, Phys. Rev. Lett. 93 (4) (2004) 247401.
[13] Y. Liu, J.S. Xue, T. Zheng, J.R. Dahn, Carbon 34 (1996) 193–200.
[14] J. Zhou, C. Booker, R. Li, X. Zhou, T.-K. Sham, X. Sun, Z. Ding, J. Am. Chem. Soc. 129 (2007) 744–745.
[15] J.E. Riggs, Z. Guo, D.L. Carroll, Y.-P. Sun, J. Am. Chem. Soc. 122 (2000) 5879–5880.
[16] Y.-P. Sun, B. Zhou, Y. Lin, W. Wang, K.A.S. Fernando, P. Pathak, M.J. Meziani, B.A. Harruff, X. Wang, H. Wang, P.G. Luo, H. Yang, M.E. Kose, B. Chen, L.M. Veca, S.-Y. Xie, J. Am. Chem. Soc. 128 (2006) 7756–7757.
[17] A.B. Bourlinos, A. Stassinopoulos, D. Anglos, R. Zboril, M. Karakassides, E.P. Giannelis, Small 4 (2008) 455–458.
[18] M.A. Lillo-Ródenas, D. Cazorla-Amorós, A. Linares-Solano, Carbon 41 (2003) 267–275.